WATER RESOURCES RESEARCH, VOL. 29, NO. 11, PAGES 3605–3614, NOVEMBER 1993

Experimental Studies of Bed Topography and Flow Patterns in Large-Amplitude Meanders 1. Observations

PETER J. WHITING[1] AND WILLIAM E. DIETRICH

Department of Geology and Geophysics, University of California, Berkeley

Large amplitude river meanders have been observed to contain multiple bars within a single loop and to exhibit planforms that are asymmetric or have subsidiary bends. Here we report experiments conducted in symmetric sine-generated meanders of large amplitude which document the bed topography, flow patterns, and sediment transport fields in such bends. Multiple pools spaced at a distance of 3–4 widths develop successively along the outer concave bank. Downstream of each pool a distinct bar lies along the inside convex bank. The series of bars overlap and appear shingled downstream; the leading edge of each bar is oblique to the channel trace and curves toward the inside bank. The first and most pronounced pool, opposite the first inner bank bar, is consistently positioned where the projection of the inner bank tangent at the upstream crossing intersects the outer bank. Successive shingled bars in the bend migrate downstream if bars arriving at the persistent first pool deliver large enough pulses of sediment to the pool to form new bars. In experiments with an erodible bank, the banks near pools are sites of accelerated retreat. This suggests that the shear stress fields engendered by these multiple features may cause the planimetric distortion seen in larger rivers.

INTRODUCTION

In his pioneering study of Japanese rivers, *Kinoshita* [1961] described two types of river meanders: meanders with two bars per channel wavelength (one bar per bend), and meanders with three or more bars per channel wavelength (more than one bar per bend). In the first case this bar was located along the convex inner bank near each bend apex, whereas in the second case, bars were in a variety of positions with respect to the planform. In the first case the meanders of low amplitude were observed to migrate consistently downstream, thus maintaining their symmetric form, whereas in the second case the meanders were of large amplitude and individual parts of these bends showed differential shift leading to complex planform growth.

The first type of meander bend has dominated researchers' attention. Field, flume, and theoretical investigations have yielded a progressively more complete understanding of these fairly symmetric and simple bends [*Dietrich*, 1987]. No comparably detailed body of research exists for the second type of meander. Nonetheless, several studies have supported Kinoshita's overall impression. *Lewin* [1972], *Hooke and Harvey* [1983], and *Thompson* [1986] all found multiple bars within single loops. Other examples have been reported, but many of the pools were associated with local curvature of the channel trace or with irregular banks [e.g., *Leopold*, 1982]. Multiple topographic undulations also have been noted in flume bends. Again, however, the additional pool or pools in a loop were often associated with a local radius of curvature minimum [*Yamaoka and Hasegawa*, 1984] or an infinitely large change in the radius of curvature due to joining a straight channel to a constantly curved channel [*deVriend and Struiksma*, 1984; *Odgaard*, 1986]. Two observations by *Zimmerman and Kennedy* [1966] and *Engelund* [1975] in a flume carving a 270° arc and in a circular annulus, respectively, showed that multiple topographic oscillations could form in long bends of constant curvature. While neither investigation documented topography in detail, the results provide unambiguous evidence that multiple bars like those described by *Kinoshita* [1961] need not be associated with local planform irregularities.

A review of theories that have been proposed to explain the development of multiple pools and bars in a bend is given in the companion paper [*Whiting and Dietrich*, this issue]. In short, the theories propose that either (1) multiple bars form from an overshoot response to the first bar/pool feature in the bend; (2) multiple bars are just alternate bars in a curved planform; or (3) multiple bars develop in response to an instability of flow through a curved planform.

In this first paper we present results from experiments designed to carefully document the basic patterns of flow, sediment transport, and boundary shear stress in elongate bends. This information is then a starting point for the second paper in which we investigate the underlying physical mechanisms that generate the multiple bar/pool features.

METHODS

Flow and bed topography in large-amplitude meander bends were studied in 25-cm-wide flume channels that followed a sine-generated curve [*Langbein and Leopold*, 1966],

$$\phi = \omega \sin [2\pi s/m].$$

The angle the centerline makes with the downvalley direction, ϕ, at point s, depends upon the angle at the inflection between bends, ω, and the proportional distance, s/m, where s is the distance downstream along the channel, and m is the total length along one waveform. The sine-generated equation was used because it gives a smoothly varying radius of curvature that reaches a single minimum at the

[1]Now at Department of Geological Sciences, Case Western Reserve University, Cleveland, Ohio.

Paper number 93WR01755.
0043-1397/93/93WR-01755$05.00

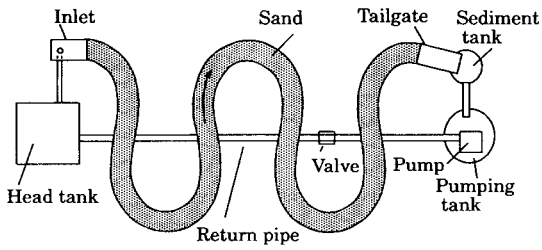

Fig. 1. Sketch of the flume and experimental setup.

apex of a symmetric bend. Use of a simple form avoids the introduction of additional planform complexity that would complicate description and interpretation of the results. Two channel configurations were studied: ω of 100° and 115° which have sinuosities of 2.69 and 4.55, respectively. The wavelength was set equal to 2.0 m (8 channel widths) because this was the length of alternate bars developed in straight 25-cm-wide channels with the same sediment and similar discharges and slopes [*Whiting and Dietrich*, 1993]. The imposed wavelength as scaled by channel width is typical of natural rivers [*Inglis*, 1949; *Leopold and Wolman*, 1957].

The channel banks were clear 0.24-cm-thick Plexiglas strips inserted into vertical sinuous slots routed into 2.86-cm-thick marine plywood sheets. The plywood sheets sat upon a raised 490 × 365 cm platform which was large enough to accommodate five bends (Figure 1). The flume was filled with 10–15 cm of sand. A well-sorted quartz sand with a median diameter of 0.062 cm was used in most runs. For this sediment, D_{16} equaled 0.044 cm and D_{84} equaled 0.077 cm; the subscripts designate the grain diameter such that 16 and 84% are finer. The critical boundary shear stress for entrainment of the median size is 3.2 dyn cm^{-2} (calculated from *Vanoni* [1964] and qualitatively confirmed by inspection).

Water discharged from the flume into a sediment-collecting tank into which a nylon mesh bag was inserted for sediment sampling. Sediment-free water spilled from the collecting tank into the pumping tank, whereupon it was raised through a 5-cm pipe to the head tank. The 0.1-m^3 head tank had a 10-cm-diameter overflow pipe that acted to maintain a constant water level in the tank, thus modulating any variation in flow transmitted from the pump. The overflow pipe returned water to the pumping tank. Water entered the flume through a 3.8-cm flexible hose connecting the inlet box to the base of the head tank. Fibrous meshes baffled the flow, but a horizontal jet formed along each bank. A metal lip across the entrance to the flume set the upstream water level. A thin plastic plate buried in the bed just downstream from the head gate limited scour. At the downstream end of the flume a tailgate set the water surface elevation and prevented net lowering of the channel bed. Bed slope through the flume was set by banking sediment to different gradients and by adjusting the headgate and tailgate. Flume discharge was adjusted with a valve along the pump line and by altering the elevation of the head tank.

Flow discharge was measured by the average time interval required to fill a calibrated bucket. Sediment discharge at the tailgate was collected in a nylon mesh bag and measured volumetrically every 5–15 min. This sediment was immediately reintroduced by hand at the flume entrance. Observations suggest that the intermittent feed caused only transitory perturbation to the flow.

Intensive study was made of the third bend because it was the farthest from the flume inlet and outlet. It is clear from repeated sketches of the bed throughout the flume that grossly similar bed features and behaviors occurred in all bends. Local sediment transport rates were measured at 2.5-cm intervals across the channel and at about half-width intervals along the channel. Three or four measurements were made at each point with a 1-cm-wide, 6-cm-long, open top brass sampler of our own construction. A raised flap at the tail of the sampler causes sediment to deposit on the sampler. While no detailed study of the accuracy of the custom sampler has been made, observation of the sampler through the clear flow gave no indication of deflected sediment trajectories nor evidence for either deposition or scour upstream of the sampler that would compromise the results. Further confidence in the local transport measurements comes from the close match between local sediment flux integrated across the channel and tailgate flux. Sediment transport directions were determined by viewing videotapes made of the bed. Videotapes of the flow littered with paper confetti were digitized to document surface flow direction and magnitude.

Water surface topography was measured with a caliper attached to a portable carriage that traversed the channel. At 2.5-cm intervals across transects spaced about 25 cm along the flume, the caliper was lowered to the water surface until a small pointer on the caliper disturbed the surface. A consistent reading required typically three to five tries. The top of the rigid bank was used as a local elevation datum. During a run the flume was drained of water intermittently to measure bed topography. Minor modification of topography occurred during the draining or reintroduction of water. The bed topography was measured with the caliper at 2.5-cm intervals across the flume, with additional measurements near the banks, and at half-channel-width intervals along the flume. During experiments the depth at the bank was monitored intermittently by tracing the bed surface on the clear channel walls. The position of scour holes and bar fronts in all bends was mapped every 5–20 min.

Table 1 presents the hydraulic conditions for each run. Average total boundary shear stress is calculated as the horizontal component of the pressure gradient force. The average local boundary shear stress is approximately the stress required to predict the observed sediment discharge using the bed load equation of *Fernandez Luque and van Beek* [1976]. The Froude number in most runs was less than 0.80, and supercritical flow was found only locally over bar tops.

BED TOPOGRAPHY IN HIGHLY SINUOUS MEANDERS

Fully Developed Form

In large-amplitude meander bends, multiple pools are found along the outer concave bank as part of a series of shinglelike bar units. Figure 2 from experiment 100-3 after 165 min and Figure 3 from experiment 115-3 after 945 min provide good examples for a discussion of the characteristic bed morphology in symmetric large-amplitude meander bends. (The experiment number gives the ω value of the meander trace and then the sequential run in this suite of

TABLE 1. Hydraulic Conditions in Experiments

Run	Width, cm	Flow Discharge, mL/ s	Flow Depth, cm	Water Surface Slope	Sediment Discharge, mL/s	Total τ_b	Local τ_b	Total τ_b/ Local τ_b	Froude Number	Width/ Depth
100-1	25.0	940	1.50	0.0060	0.630	8.8	5.7	1.55	0.65	17
100-2	25.0	1180	1.58	0.0044	0.276	6.8	5.0	1.36	0.76	16
100-3	25.0	1180	1.66	0.0040	0.171	6.5	4.4	1.48	0.70	15
115-1	25.0	1260	1.87	0.0064	1.200	11.7	7.5	1.57	0.63	13
115-2	25.0	1060	1.62	0.0057	0.521	9.1	5.5	1.65	0.66	15
115-3	25.0	1000	1.60	0.0045	0.309	7.1	4.7	1.50	0.63	16
115-4	38.9	1070	1.02	0.0043	0.165	4.3	4.3	1.00	0.85	38
115-5	52.0	1070	0.81	0.0063	2.790	5.0	4.7	1.07	0.90	64
115-6	45.7	1042	1.11	0.0054	0.665	5.9	5.7	1.03	0.62	41
115-7	12.5	650	1.63	0.0051	0.480	8.2	4.7	1.74	0.80	8
115-8	12.5	422	2.49	0.0041	0.370	10.0	6.3	1.59	0.27	5

experiments.) In experiment 100-3 (Figure 2), pools along the concave bank are centered at sections 1.45 and 1.61; in 115-3 (Figure 3), they are at sections 1.38, 1.50, 1.62, and 1.72. In both cases the pools within the relatively constant curvature portion of each bend are found only along the outer bank, and these pools are deeper than those downstream in the approximately straight reaches between bends. The first well-defined pool along the outer bank in each bend is located upstream of the bend apex of the loop. (The bend apex is at section 1.50; the section number corresponds to the s/m value.) For these largest-amplitude bends the first pool is located approximately where the projection of the tangent to the inner bank at the upstream inflection (crossing) between bends (at section 1.25) intersects the outer bank. This first pool is often the deepest of the successive pools and at its maximum is 2–3 times as deep as the average flow.

Each pool is part of a bar unit similar to that well known from straight channels and low-amplitude meanders. In experiment 100-3 (Figure 2) a downstream widening and shoaling surface extends from the pool near 1.45. The upstream edge of this surface is the slip face of the point bar at the bend entrance curving from section 1.40 along the concave bank to 1.50 along the convex bank. The downstream edge of the shoaling surface is defined by a similarly curving slip face into the second pool; this second edge extends from sections 1.55 to 1.67. In experiment 115-3 (Figure 3) the pattern repeats for a third time in the longer bend.

As the radius of curvature increases rapidly out of the constantly curved portion of the bend into the relatively straight channel between bends, depositional lobes are no longer exclusively wrapped inward (Figure 2 and 3) and instead extend further downstream along the same banks as the scour. In addition, though not well expressed, scour holes are also found along the inner bank; for example, at section 1.68 in Figure 2. The features in this less-curved reach have the morphology of alternate bars, but are not as long (4–6 channel widths) as fully developed alternate bars in

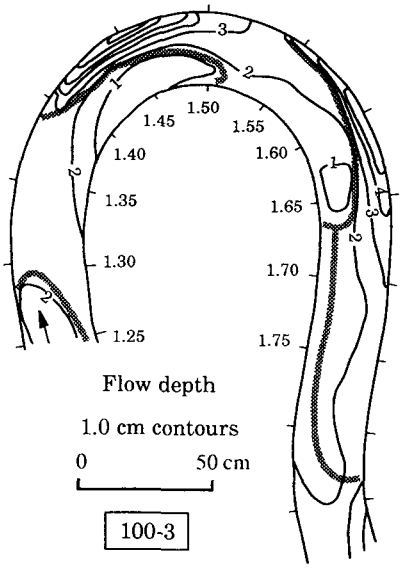

Fig. 2. Bed topography in experiment 100-3 when flow was interrupted after 165 min. The stippled lines mark the steep edge of the bar tops as both observed and measured during surveys. In many, but not all cases, the steep slip face can be discerned from the contours.

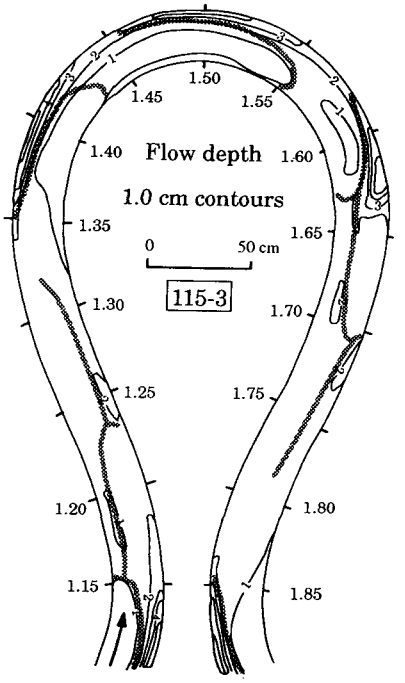

Fig. 3. Bed topography of experiment 115-3 when flow was interrupted after 945 min. The stippled lines mark the edge of bars.

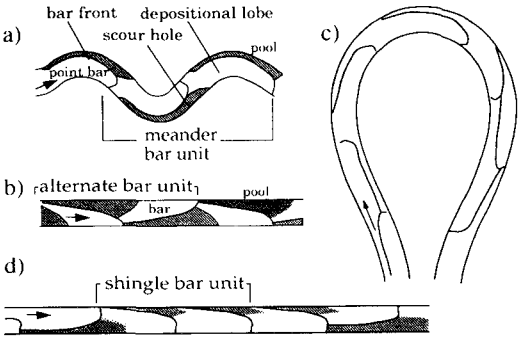

Fig. 4. A comparison of (*a*) the basic bar unit of low-amplitude meanders, (*b*) alternate bars in straight channels, and (*c*) shingle bars in large-amplitude meanders. The general morphology seen in Figure 4*c* is "unwound" in Figure 4*d* for comparison with a true alternate bar sequence (Figure 4*b*).

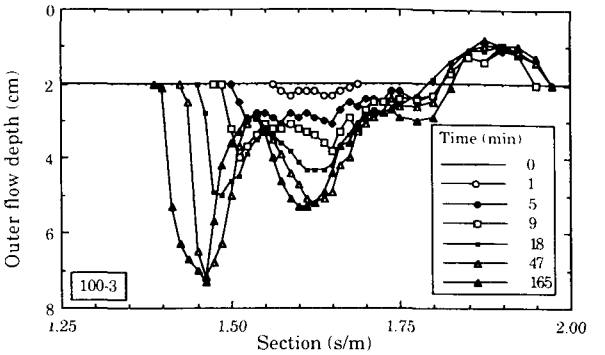

Fig. 5. The temporal development of scour along the concave outer bank as recorded by frequent traces of the bed surface on the clear flume walls. The upstream propagating scour appeared to exhibit oscillations in depth early in its development (i.e., at 5 min) which were amplified as the scour approached the bend apex. (Data are from experiment 100-3).

straight channels (~8 channel widths between pools lying along the same bank).

So, as in straight channels and low-amplitude meanders, there is a series of pools and shoals in large-amplitude bends. But unlike point bars and pools in a low-amplitude meander (Figure 4*a*) and alternate bars in a straight channel (Figure 4*b*), these bars do not lie on opposite banks in succession down the channel. In the persistently curved reaches (Figure 4*c*) the pools are always along the outer bank, and the shoals are along the inner bank. It is as if the effect of curvature has been to sweep the depositional lobes inward. The series of bar margins all of which curve toward the right bank gives the bed in the bend a "shingled" appearance; like tiles on a roof the bars overlap (Figures 3 and 4). Illustrating this point, a schematic representation of the bend and bars is reproduced in Figure 4*c* and then is uncoiled as Figure 4*d*. To distinguish this distinct morphology from that of alternate bars, we call these overlapping features "shingle bars." This pattern of successive bars with the same sense of curvature has been called "C type" in Japan [*Kinoshita*, 1957]. The spacing of the shingle bars as measured by the streamwise distance between pools is 86 and 100 cm in the 100° and 115° bends. Scaled by the channel width, these lengths correspond to 3.4 and 4.0, respectively.

Bed Evolution to Stable Topography

The temporal development of topography was monitored by repeatedly tracing the sediment-water interface on the clear outer bank. Using experiment 100-3 as an example, it took about 150 min for the morphology to become fully developed (Figure 5). Scour developed initially near section 1.62, along the bank that connects the upstream bend's outer bank to the downstream bend's inner bank. This is the stretch of channel where we expect the steepest water surface slopes [*Dietrich*, 1987] and the largest local boundary shear stresses. This pool lengthened rapidly upstream and downstream, and scoured sediments were in large part deposited on the point bar along the convex bank in the downstream bend (between sections 1.85 and 1.95). At 9 min, when the tip of the scour had advanced to the bend apex, the outer bank scour had two distinct pools located at sections 1.52 and 1.65. By 47 min the upstream pool had shifted upstream of the bend apex and both had deepened. During the next 120 min the pools shifted slightly, finally stabilizing near 1.46 and 1.60, with an intermediate shoal near 1.53. During the upstream propagation of the pools the bed at the site of the central shoal was never deeply incised. Pools lowered into their positions and in so doing defined the central hump near section 1.53. The bed in experiment 115-1 evolved similarly, and the incised positions were near sections 1.39 and 1.50.

Bar Dynamics

In experiments 100-3 and 115-3 the shingle bars within the central part of the bend were static after their original development (Figures 2 and 3). A convenient way to represent the positions of the bars is by the position of the scour holes along the left bank; for the bend centered at section 1.5, the left bank corresponds to the concave outer bank. In experiment 115-3 the pools of the stationary bar units were located at 1.38, 1.50, and 1.62 (Figure 6). Bars in the

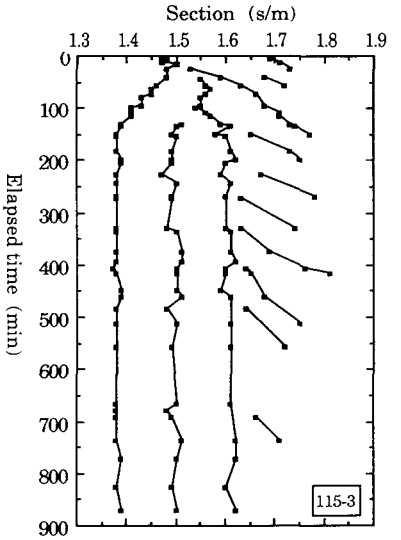

Fig. 6. Migration of bars as indicated by the shift in the position of outer bank pools occurs only within the relatively straight portions of the planform (experiment 115-3). No migration was observed in the nearly constantly curved portion of the bend ~1.35–1.65. The bed topography after 945 min is shown in Figure 3.

straighter reach between bends were observed to migrate but were eventually lost below section 1.85 as they propagated onto the point bar at the entrance to the next bend.

In other cases, bars within the central part of the bend migrated. In experiment 115-1 the shingle bars translated as indicated by the downstream shifting position of pools along the left bank (Figure 7). The shingle bars within the bend were initially stable in position but with the arrival at 50 min of the first scour hole (and corresponding bar) that had migrated through the straight upstream reach, the entire train of pools within the bend, with the exception of the first pool, began to shift downstream. Subsequent arrivals of pools (and bars) also appeared to trigger movement of the shingle bars. The pools accelerated when they moved into the nearly straight reach beyond section 1.65. When bars that previously had been attached to the inside bank (i.e., shingled) entered the straight reach, the leading edge of the bar closer to the left (concave bank) migrated faster than the bar edge closer to the convex bank. This gradually transformed the bars such that the pool and depositional lobe lay along the same bank. This is the geometry observed for alternate bars (Figure 4*b*).

The migration of the bars in the curved portion of the channel is associated in time with the arrival of the first well-defined bar after its migration through the relatively straight upstream reach. While from the migration of this and other bars it might appear reasonable to connect the bars upstream of 1.39 to those below 1.39 (Figure 7), detailed observations and tracings show that the arriving bars did not propagate through the deep pool adjacent to the fixed point bar. An incipient bar was generated by the arrival of the upstream bar. Figure 8 presents an instantaneous view of topography during the development of such a new scour hole (or more appropriately, the formation of a new bar) along the outer bank. The new bar's leading edge curves from near 1.44 along the concave bank to 1.48 along the convex bank. The new feature was initially a migrating swell in the otherwise deep pool, but as this new bar grew in height and length, it developed the obliquity that distinguished it as a shingle bar. The arrival from upstream of a migrating bar partially filled the first pool, and then erosion of this material

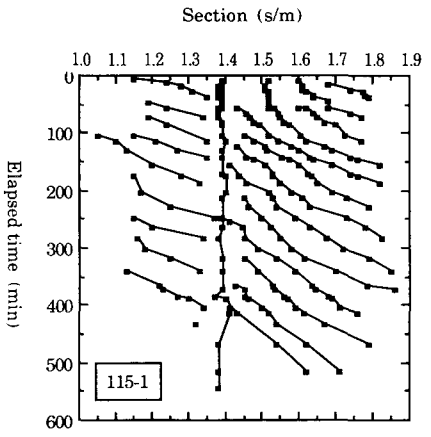

Fig. 7. Migration of bars within the bend and straight portions of the channel is indicated by the shift in the position of outer bank pools. The arrival at the persistent pool (1.38) of the first bar from upstream appeared to trigger the migration of bars within the bend. (Data are from experiment 115-1).

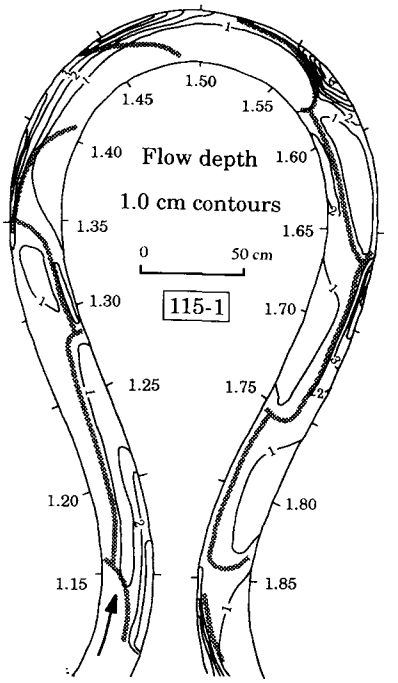

Fig. 8. Bed topography in 115-1 during formation of new bar front at section 1.44 after 105 min. The slip face marking the edge of this new bar near the inner bank, while clearly visible, is too small to be resolved by the 1-cm contours.

appears to have created the new and growing feature in the downstream part of the persistent pool. Either this new feature modified the sediment flux downstream and in so doing altered the stability of downstream features, or the partial filling of the first pool altered flow through the remainder of the bend, causing the entire train of bars to begin moving. For either scenario the magnitude of the perturbation of sediment supply to the pool should depend upon the local boundary shear stress and the relief of migrating bars. It is indeed the case that shingle bar migration within the bend occurred when relief and stresses were large (Table 1). In experiment 115-1 where bars migrated, topographic relief (Figure 8) was greater than in experiment 115-3 where bars did not migrate (Figure 3), and furthermore total boundary shear stress in 115-1 was 60% greater than in 115-3.

The consequence of bar migration through the bend is that depth at a point along the outer bank varies, but in a manner that is somewhat unexpected. In experiment 115-2 (Figure 9), minimum depths associated with the top edge of the advancing bar front are approximately equal to the mean flow depth except at the bend entrance where the first pool never completely fills with sediment. Maximum flow depths associated with the migrating pools do not uniformly decrease from the first pool. Locally greater scour depths were observed when bars were at positions near 1.43 and 1.56. The spacing of these sites of maximum scour depths is not the same as the bar spacing, nor are these the sites of stable pools (as in experiment 115-3 where pools were located at 1.38, 1.50, and 1.62). In experiment 100-2 the deepest scour with migration of pools was at 1.43 and 1.57, but in experiment 100-3 where bars were not migrating, the pools were located at 1.45 and 1.61.

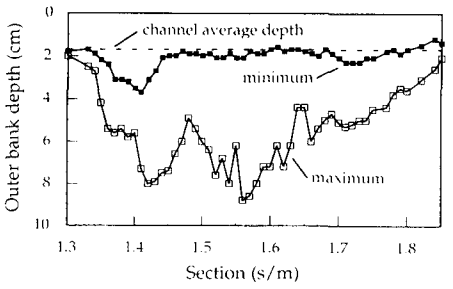

Fig. 9. Maximum and minimum depth along the flume during the propagation of bars in experiment 115-2. The first pool never completely fills with sediment during migration. The locations of maximum scour, 1.42 and 1.57, are not the sites where bars stabilized in experiment 115-3. It appears some amplification of scour occurs at certain locations in the planform.

Position of Pools

We hypothesize that the position of the upstream and most persistent pool is controlled by the outward forcing of flow due to curvature and point bar growth. These two factors combine to cause the high-velocity core to shift toward the outer bank approximately along a line tangent to the inner bank at the crossing between bends (e.g., at section 1.25). A line describing this geometry for various sine-generated planforms [*Whiting and Dietrich*, 1993] is plotted in Figure 10. The larger the bend angle and the narrower the channel with respect to the cartesian wavelength, the further upstream is the pool. Our data and other sine-generated flume data from *Hooke* [1975], *Gottlieb* [1976], *Yamaoka and Hasegawa* [1984], and *Whiting and Dietrich* [1993] closely follow the geometric relation.

While the stable position of the first pool can be predicted on the basis of the planform, the location of subsequent pools is not tied directly to particular sites within the bends. In 100° bends without migrating shingle bars, stable pools flanked the bend apex (Figure 2), while in 115° bends without migrating bars, a stable pool was centered at the bend apex with a pair of pools symmetrically flanking the pool at the apex. In any experiment the pools were identically spaced along the concave bank at intervals averaging 3.4–4 channel widths in the 100° and 115° experiments, respectively. In our experiments and in those experiments with constant curvature of the channel trace [*Zimmerman and Kennedy*, 1966; *El-Khudairy*, 1970; *Engelund*, 1975; *Kikkawa et al.*, 1976], pools were spaced at 3- to 5-channel-width intervals along the concave bank (Figure 11). In several experiments discussed more completely in our companion paper [*Whiting and Dietrich*, this issue], halving channel width doubled the spacing of bars, the result of which was that for both planforms bars were located at the same site as in the wider channel.

FLOW, SEDIMENT TRANSPORT, AND SHEAR STRESS FIELDS

To analyze the processes giving rise to multiple bar formation, we mapped the patterns of flow, water surface slopes, shear stress, and sediment transport in each experiment. The stationary bars in experiments 100-3 or 115-3 make them convenient, if not completely representative, examples for discussion. We present results from 115-3 because the additional bar in these longer bends provides a more compelling illustration of the periodic behavior of flow, sediment transport, and shear stress.

The bed topography of experiment 115-3, first shown in Figure 3, is reproduced in Figure 12*a*. Pools are located along the outer (concave) bank near sections 1.38, 1.50, 1.62, and 1.72, and the series of bars attach to the inner (convex) bank. Only the pool at section 1.72 is nonstationary. The water surface topography is shown in Figure 12*b*. At the inflection between bends (sections 1.25 and 1.75), downstream water surface slopes are steep and cross-stream slopes rather small. Downstream to section 1.38, downstream water surface slope decreases along both the inner and outer bank. Beyond the point bar at 1.40, inner bank water surface slope steepens. Cross-stream slopes with a tilt toward the inner bank develop by section 1.33. This tilt is maintained through the remainder of the bend to near 1.65, but its strength varies through the bend. Past the bend apex (section 1.50), beyond which the radius of curvature lengthens, the downstream water surface slope generally decreases along the inner bank and increases along the outer bank. Local water surface highs along the outer bank (sections 1.39, 1.50, and 1.63) occur over the upstream portion of the pools as flow decelerates in the deeper flow. These free surface effects are significant and modify the overall pressure gradient field, as will be discussed below.

The pattern of surface flow, as indicated by the trace of the videotaped confetti, is shown in Figure 12*c*. The largest surface velocities are found along the inner bank near the inflection between bends. A strand of higher-velocity fluid

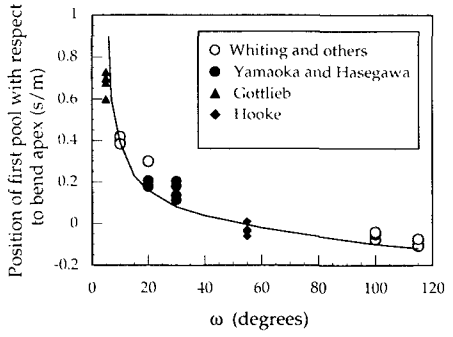

Fig. 10. Geometric prediction of position of initial outer bank pool as a function of wavelength-to-width ratio and comparison with data.

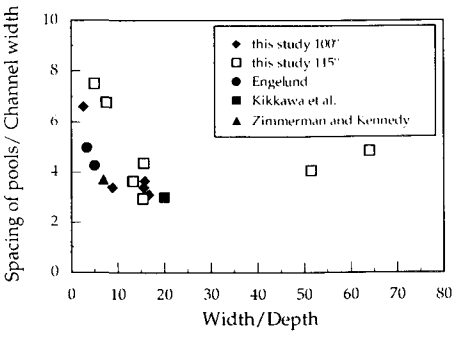

Fig. 11. Bar wavelength to channel width ratio compared to channel width-to-depth ratio.

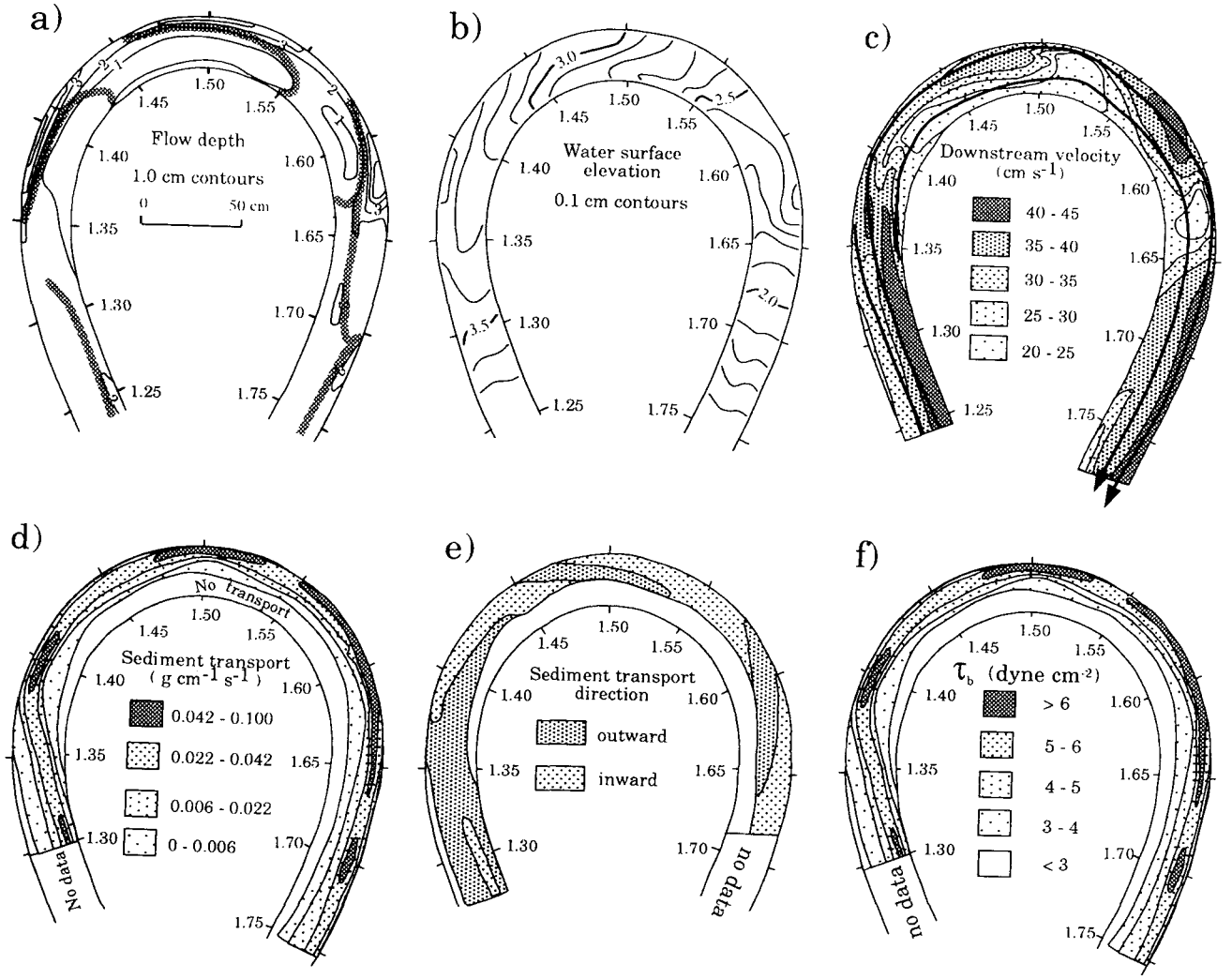

Fig. 12. (*a*) Bathymetry, (*b*) water surface elevation, (*c*) surface flow direction and magnitude, (*d*) local sediment transport rate, (*e*) sediment transport direction, and (*f*) local boundary shear stress for experiment 115-3. In Figure 12*c* the heavy lines follow paths of selected surface floats.

crosses to the outer bank past the first pool and remains near the outer bank until the next bend. Superimposed upon this pattern of higher velocity along the outer bank (past the first pool) are local flow accelerations over topography. For example, at sections 1.47, flow accelerates over the edge of the bar front where flow spills into the laterally adjacent deepest part of the pool. Outward surface flow over the point bar is discernable by section 1.32. A surface float which at 1.32 is at the channel centerline is within 2 cm of the outer bank by section 1.40. Past the initial pool, surface flow near the outer bank is alternately inner bank and outer bank directed; that is, over the downstream part of each pool and upstream part of each shoal, surface flow is directed slightly inward, while over the downstream part of each bar top and the upstream part of each pool, surface flow is directed outward. This observation is particularly important because it shows that the effect of the oblique bar front, which is to direct the flow inward, overwhelms the centrifugal force–induced outward flow expected in a curved channel. *Yamaoka and Hasegawa* [1984] also observed inward flow in the widening downstream portion of the first pool in a bend.

Sediment transport is concentrated along the inner bank in the upstream part of the bend, crosses to the outer bank in the first pool, and remains along this bank to the next bend (Figure 12*d*). The zone of active transport widens slightly over the shallow bar top between pools but does not extend to the inner bank. Local transport rates are greatest on the side slopes in the upstream portion of each pool. Sediment transport trajectories as determined from videotapes are toward the outer bank over the first bar and into the pool, toward the inner bank in the first pool and along the slip face, and then toward the outer bank again near the active part of the top of the second oblique bar front (Figure 12*e*). This general pattern is repeated downstream over each successive bar and is similar to the pattern identified for single bar bends [*Dietrich and Smith*, 1984].

We estimated the local boundary shear stress by inverting the bed load equation of *Fernandez Luque and van Beek* [1976] to solve for the stress required to predict the observed sediment flux,

$$\tau_b = (\rho_s - \rho)gD\left\{\left[\frac{Q_{bl}}{5.7\rho_s}\frac{1}{\left[gD^3\left(\frac{\rho_s-\rho}{\rho}\right)^{0.5}\right]}\right]^{0.666} + 0.032\right\}$$

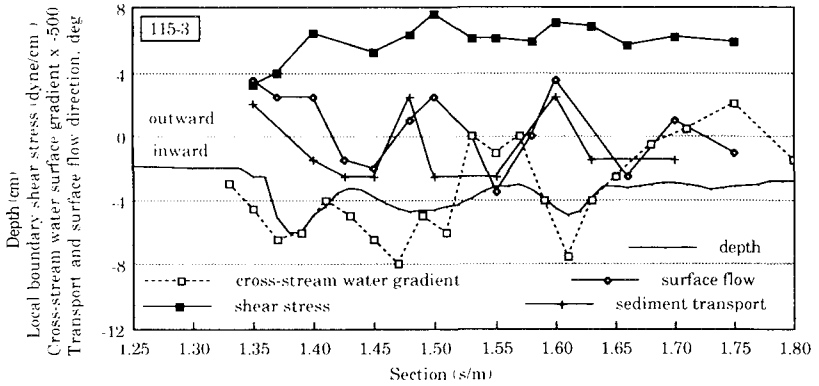

Fig. 13. Variation in cross-stream water surface gradient, surface flow directions, sediment transport directions, shear stress, and flow depth along a longitudinal transect 2.5 cm from the outer bank in experiment 115-3. Outward is toward the concave bank.

Q_{bl} is the sediment flux, ρ_s and ρ are the density of the sediment and water, respectively, g is the gravitational acceleration, D is the median grain diameter, and τ_b is local boundary shear stress. The critical dimensionless boundary shear stress for sediment entrainment is 0.032 [*Vanoni*, 1964]. We did not attempt to account for the modification of transport rates by the sloping bed. The corridor of high boundary shear stress tracks the sediment flux and crosses to the outer bank at the first pool (Figure 12*f*) as can be expected since no significant lateral variation in grain size occurred in this well-sorted sediment. Maximum stresses in the upstream part of the pools are up to 2.5 times the critical boundary shear stress for entrainment ($\tau_{cr} = 3.2$ dyn cm^{-2}).

Figure 13 provides a summary of the hydraulic factors through the same bend presented above along a longitudinal profile 2.5 cm from the outer (concave) bank. At the bend entrance, surface flow is outward as seen by the trajectory of surface floats. Injection of dye showed that near-bed flow is outward as well: a pattern similar to that due to bar topographic forcing recognized in single-bar bends [*Dietrich and Smith*, 1983]. A local water surface high near 1.38 steepens the downstream and the cross-stream water surface slopes (Figure 12*b*). Concurrently, sediment transport vectors, which had been aligned with the outward flow, turn inward toward the convex bank. Local boundary shear stress increases below section 1.35, reaching a maximum in the deepest part of the pool at 1.40. Outward surface flows continue to section 1.40. Past section 1.40, local boundary shear stress drops, depth decreases, and both sediment transport and surface flow are directed toward the inner bank. At section 1.45, depth increases again as local boundary shear stress increases. Surface flow and sediment transport directions are outward into the deepening pool by 1.48. In the lee of the bar front at 1.50, sediment transport vectors turn inward while surface flow is still outward. Shoaling past 1.50 is associated with decreasing shear stress and inward surface flow. This is spatially associated with a second strong cross-stream water surface tilt found at 1.50. Over the middle of the shoaling reach (1.55), both surface flow and near-bed transport are again directed toward the inner bank. By the point at which depth reaches its minimum at 1.58, surface flow has turned outward again. Depth and shear stress increase beyond section 1.58 to near 1.64. As the depth decreases in the downstream part of the pool, surface flows again become directed inward.

The periodically disturbed bed topography in this elongate bend reaches equilibrium when boundary shear stress divergence tied to systematic periodic streamwise shoaling and deepening is compensated by net cross-stream sediment transport. Specifically, deposition in reaches of decreasing boundary shear stress along the outer bank is prevented by the inward transport of sediment, and erosion in reaches of increasing boundary shear stress is prevented by net outward transport of sediment. Cross-stream sediment transport toward the inner bank results from strong inward flow that develops in the pools in the lee of the oblique bar front. Cross-stream sediment transport toward the outer bank results from flow forced outward by shoaling topography. The rapid flow deceleration in the deepening and widening pool in the lee of the bar front is sufficiently large that the cross-stream pressure gradient force is greater than the centrifugal force and turns the flow through the entire water column inward. This is a critical observation and can be seen near 1.42 in both Figures 12*c* and 13. The effect of the strong local cross-stream pressure gradient is to give the flow an orientation that is not adapted to the downstream conditions of continuously curving banks. The outward tilt to the bed surface created by the cross-stream convergence of sediment transport eventually redirects the flow back toward the continuously curving outer bank, with the consequent outer bank superelevation, cross-stream and downstream water surface steepening, and scour.

These observations are similar to the conclusions of *Dietrich and Smith* [1983, 1984] for the equilibrium topography in single-bar bends. In the bends described here, the repeated pool and bar topography emerges from repeated "topographic steering" [*Nelson and Smith*, 1989] which forces flow and sediment transport into the pool from the bar top and forces flow and sediment out of the pool in the lee of the oblique bar front.

BANK EROSION EXPERIMENT

The demonstration that elongate rigid-walled bends develop a series of overlapping bars which systematically force a variation in near-bank shear stress suggests that given

erodible banks these features could cause locally enhanced bank erosion. To investigate whether the topographically driven stress patterns could lead to local bank erosion which, in turn, might lead to the development of the distinctive planforms of large-amplitude bends, we removed the rigid outer wall from section 1.30 to 1.82 in one of the bends. In its place, loose sand of the same size as the bed was filled to the level of the water surface.

The pattern of bank erosion starting from shingle bar topography (experiment 115-4) and from an initially flat bed (experiment 115-6) was monitored until the bank margins approached the edge of the flume platform. The evolution of the channel trace starting from an initially flat 25-cm-wide bed with erodible bank material is traced in Figure 14. At each time shown on the figure, the channel width at approximately 20-cm intervals was measured. By 36 min, two distinct sites (marked by tick marks) of locally greater bank retreat emerged; the first upstream of the bend apex past the developing point bar, and a second downstream of the apex opposite a second shingle bar top attached to the inner bank. With continued widening at 50 min, material that was eroded out of the first pool and from the outer bank and then swept toward the inner bank lengthened this shingle bar. Bank erosion spatially associated with the outer bank pool laterally adjacent to this shingle bar shifted downstream with the lengthening bar (Figure 14). With yet further widening, the second shingle bar extended downstream into the straighter reach, and the distance between sites of locally greater bank retreat lengthened. As this happened, the downstream bar no longer remained attached to the inner bank and by 62 min shifted toward the channel center. A similar pattern of bank erosion and planform evolution was observed starting from a bed previously molded into a series of shingle bars in a channel with a rigid bank. Outer bank retreat was most rapid upstream of the bend apex near section 1.94 (experiment 115-4). The erodible bank experiments do not show as many bars per bend as rigid wall experiments, and bars tend to become less shingled as the channel widens.

It is clear that bed and bank deformation skews the originally symmetric sine-generated planform (Figure 14). At the bend entrance, outer bank retreat acts to lengthen a segment of relatively straight flow. The net effect of the erosion upstream of the apex of the originally symmetric trace is to give the bends an asymmetry similar to the shape of the letter D; the straight channel forms the vertical stroke of the letter. Enhanced erosion associated with the tip of the second bar in the bend gives a second local radius of curvature minimum which could lead to a subsidiary bend. These experiments show that a large-amplitude bend could become asymmetric by flow that crosses to the outer bank upstream of the apex rather than by the delayed crossing of the high-velocity core as proposed by *Carson and Lapointe* [1983], or it could become compound by the pattern of erosion forced by the multiple bars.

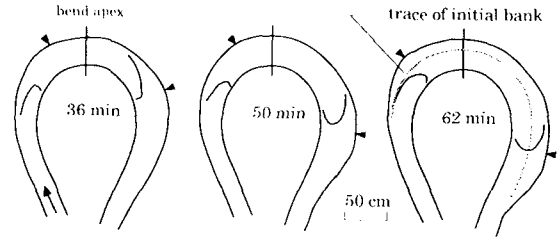

Fig. 14. Local bank retreat associated with the position of bars distorts the originally symmetric channel trace in experiment 115-6. The small ticks along the outer bank are the positions of maximum local bank retreat. The inner bank is inerodible.

CONCLUSIONS

In summary, we observe the following: (1) the bed in the nearly constant curvature portion of symmetric large-amplitude bends is deformed into a series of shingled bars with pools along the concave bank and depositional lobes along the inner bank; (2) these shingle bars have a spacing of 3.5–4 channel widths except in very narrow channels; (3) the first pool in the bend is fixed and is located near where the inner bank tangent intersects the outer bank, (4) other shingle bars may migrate through the bend and into the nearly straight reach between bends, (5) shingle bars migrating out of the nearly constantly curved part of the bend into the straighter reach connecting bends develop into alternate bars, which, when they reach the entrance of the downstream bend, deliver a "package" of sediment that develops into a new bar in the downstream bend, (6) emergence of the shingle leads to significant local perturbations in flow, boundary shear stress, and sediment transport fields, (7) over the nonmigrating shingle bars there is a balance between boundary shear stress divergence and cross-stream sediment transport, and (8) locally enhanced bank erosion that deforms the channel trace occurs in association with the periodic topography.

The observation that multiple pools develop in large-amplitude symmetric bends with a single radius of curvature minimum, taken with the results from the erodible bank experiments, demonstrates that bed deformation seen in elongate meander loops may lead to planform elaboration. The pools are part of larger channel-wide features that appear similar in form to alternate bars in straight channels with the important difference that the persistent curvature of large-amplitude meanders causes successive pools to lie along the concave bank and successive shoals to lie along the convex bank.

Acknowledgments. Gary Parker made suggestions about the experimental design and provided translations Kinoshita's work. We benefited from discussions with Luna Leopold, Jon Nelson, Giovanni Seminara, J. Dungan Smith, and Marco Tubino. We appreciate the comments of two anonymous reviewers. Acknowledgment is made to the donors of the Petroleum Research Fund administered by the American Chemical Society for support of this research: ACS-PRF-18427-AC2 to W. E. D. and ACS-PRF- 14520-AC2 to Luna B. Leopold.

REFERENCES

Carson, M. A., and M. F. Lapointe, The inherent asymmetry of river meander planform, *J. Geol.*, *91*, 41–55, 1983.

deVriend, H. J., and N. Struiksma, Flow and bed deformation in river bends, in *River Meandering: Proceedings of the Conference, Rivers '83*, edited by C. M. Elliot, pp. 810–839, American Society of Civil Engineers, New York, 1984.

Dietrich, W. E., Mechanics of flow and sediment transport in river bends, in *River Channels: Environment and Process, Inst. Br. Geogr. Spec. Publ.*, vol. 18, edited by K. S. Richards, pp. 179–227, Blackwell Scientific, Boston, Mass., 1987.

Dietrich, W. E., and J. D. Smith, Influence of point bar on flow

through meander bends, *Water Resour. Res.*, *19*, 1173–1192, 1983.

Dietrich, W. E., and J. D. Smith, Bedload transport in a river meander, *Water Resour. Res.*, *20*, 1355–1380, 1984.

El-Khudairy, M., Stable bed profiles in continuous bends, Ph.D. dissertation, 103 pp., Univ. of Calif., Berkeley, 1970.

Engelund, F., Instability of flow in a curved alluvial channel, *J. Fluid Mech.*, *72*, 145–160, 1975.

Fernandez Luque, R. F., and R. van Beek, Erosion and transport of bed-load sediment, *J. Hydraul. Res.*, *14*, 127–144, 1976.

Gottlieb, L., Three-dimensional flow pattern and bed topography in meander channels, *ISVA Ser. Pap. 11*, Tech. Univ. Denmark, Copenhagen, 1976.

Hooke, J. M., and A. M. Harvey, Meander changes in relation to bend morphology and secondary flow, in Modern and Ancient Fluvial Systems, edited by J. D. Collinson and J. Lewin, *Spec. Publ. Int. Assoc. Sedimentol.*, *6*, 121–132, 1983.

Hooke, R. L., Distribution of sediment transport and shear stress in a meander bend, *J. Geol.*, *83*, 543–565, 1975.

Inglis, C. C., The behavior and control of rivers and channels, *Res. Publ. Indian Waterw. Exp. Stn. Poona*, *13*, 2 vol., 1949.

Kikkawa, H., S. Ikeda, and A. Kitagawa, Flow and bed topography in curved open channels, *J. Hydraul. Div. Am. Soc. Civ. Eng.*, *102*, 1327–1342, 1976.

Kinoshita, R., On the formation of river dunes, an observation of the meandering state (in Japanese), *Trans. Jpn. Soc. Civ. Eng.*, *42*, 1–21, 1957.

Kinoshita, R., An investigation of channel deformation in the Ishikari River (in Japanese), report, Bur. of Resour., Dep. of Sci. and Technology, 174 pp., Tokyo, 1961.

Langbein, W. B., and L. B. Leopold, River meanders, a theory of minimum variance, *U.S. Geol. Surv. Prof. Pap.*, *422-H*, 15 pp., 1966.

Leopold, L. B., Water surface topography in river channels and implications for meander development, in *Gravel-Bed Rivers*, edited by R. D. Hey, J. C. Bathurst, and C. R. Thorne, pp. 359–383, John Wiley, New York, 1982.

Leopold, L. B., and M. G. Wolman, River channel patterns, braided, meandering, and straight, *U.S. Geol. Surv. Prof. Pap.*, *282-B.*, 1957.

Lewin, J., Late stage meander growth, *Nature*, *240*, 116, 1972.

Nelson, J. M., and J. D. Smith, Evolution and stability of erodible channel beds, in *River Meandering*, *Water Resour. Monogr. Ser.*, vol. 12, edited by S. Ikeda and G. Parker, pp. 321–378, AGU, Washington, D. C., 1989.

Odgaard, A. J., Meander flow model, I, Development, *J. Hydraul. Eng.*, *112*, 1117–1136, 1986.

Thompson, A., Secondary flows and the pool-riffle unit, a case study of the process of meander development, *Earth Surf. Processes Landforms*, *11*, 631–641, 1986.

Vanoni, V. A., Measurements of critical boundary shear stress for entraining fine sediments in a boundary layer, *Rep. KH-R-7*, 47 pp., W. M. Keck Lab. of Hydraul. and Water Resour., Calif. Inst. of Technol., Pasadena, 1964.

Whiting, P. J., and W. E. Dietrich, Experimental constraints on bar migration through bends: Implications for meander wavelength selection, *Water Resour. Res.*, *29*, 1091–1102, 1993.

Whiting, P. J., and W. E. Dietrich, Experimental study of bed topography and flow patterns in large-amplitude meanders, 2, Mechanisms, *Water Resour. Res.*, this issue.

Yamaoka, I., and K. Hasegawa, Effects of bends and alternating bars on meander evolution, in *River Meandering: Proceedings of the Conference*, *Rivers '83*, edited by C. M. Elliot, pp. 783–793, American Society of Civil Engineers, New York, 1984.

Zimmerman, C., and J. F. Kennedy, Sediment transport and bedforms in laboratory streams of circular planform, report, pp. 1–7, Int. Assoc. Hydraul. Res., Delft, Netherlands, 1966.

W. E. Dietrich, Department of Geology and Geophysics, University of California, Berkeley, CA 94720.

P. J. Whiting, Department of Geological Sciences, Case Western Reserve University, 10900 Euclid Avenue, Cleveland, OH 44106.

(Received January 4, 1993;
revised June 7, 1993;
accepted June 22, 1993.)